



HAL
open science

The 'where' and the 'when' of the BOLD response to pain in the insular cortex. Discussion on amplitudes and latencies.

Florence B. Pomares, Isabelle Faillenot, Roland Peyron, Fabrice Guy Barral

► To cite this version:

Florence B. Pomares, Isabelle Faillenot, Roland Peyron, Fabrice Guy Barral. The 'where' and the 'when' of the BOLD response to pain in the insular cortex. Discussion on amplitudes and latencies.. NeuroImage, 2013, 64, pp.466-75. hal-00793562

HAL Id: hal-00793562

<https://hal.science/hal-00793562>

Submitted on 22 Feb 2013

HAL is a multi-disciplinary open access archive for the deposit and dissemination of scientific research documents, whether they are published or not. The documents may come from teaching and research institutions in France or abroad, or from public or private research centers.

L'archive ouverte pluridisciplinaire **HAL**, est destinée au dépôt et à la diffusion de documents scientifiques de niveau recherche, publiés ou non, émanant des établissements d'enseignement et de recherche français ou étrangers, des laboratoires publics ou privés.

The 'where' and the 'when' of the BOLD response to pain in the insular cortex.

Discussion on amplitudes and latencies.

Florence B Pomares^{a, b, c, d}, Isabelle Faillenot^{a, b, c, e}, Fabrice Guy Barral^{b, c, f}, Roland Peyron^{a, b, c, d}

^a Central Integration of Pain, Neuroscience Research Center, U1028 INSERM, F-42023, France;

^b Université de Lyon, Saint-Etienne, F42023, France;

^c Jean Monnet University, Saint-Etienne, F-42023, France;

^d Department of Neurology and Pain Center, University Hospital, Saint-Etienne, F-42055, France;

^e CMRR Unit, University Hospital, Saint-Etienne, F-42055, France;

^f Department of Radiology, University Hospital, Saint-Etienne, F-42055, France;

Corresponding author: Florence B Pomares

Address: Department of Neurology, Hopital Nord,

CHU Saint-Etienne, Avenue A. Raimond,

F-42055 Saint-Etienne cedex 2, France

Tel: +33 477 829 031

Fax: +33 477 120 543

E-mail address: florence.pomares@univ-st-etienne.fr

Abstract

The operculo-insular cortex has been recently pointed out as the main area of the pain matrix to be involved in the integration of pain intensity. This fMRI study specified the pattern of response to laser stimuli by focusing on this cortical area, by optimizing the temporal sampling and by investigating pain-specific differences in the amplitudes and latencies of the BOLD responses. Canonical and temporal derivative hemodynamic response function (HRF) and finite impulse response (FIR) modeling provided consistent results. Amplitude of BOLD response discriminated painful from non-painful conditions in posterior and mid-insular cortex, bilaterally. Pain conditions were characterized by a shortened latency (as compared to non-painful conditions) in the anterior insula and in the anterior midcingulate cortex. In the functional organization of the insula, these results suggest a double dissociation that can be summarized as the 'where' and the 'when' of the BOLD response to pain. While discriminative processes on the amplitude of the BOLD response concern the posterior and the mid-insular cortex, shortened latency of the response is observed in the anterior insula specifically during painful conditions.

Key-words

fMRI; insular cortex; laser stimulation; HRF; pain

Abbreviations

AAL, Automatic Anatomical Labeling; ACC, Anterior Cingulate Cortex; aMCC, anterior Middle Cingulate Cortex; ASG, Anterior Short Gyrus; AIC, Anterior Insular Cortex; FIR, Finite Impulse Response; Fmid, middle Frontal gyrus; HRF, Hemodynamic Response Function; IC, Insular Cortex; Ig, granular Insula; LEP, Laser-Evoked Potential; MSG, Middle Short Gyrus; NP, Non-Painful stimulus; OP, Parietal Operculum; P, Painful stimulus; PIC, Posterior Insular Cortex; PostCG, Posterior Central insular Gyrus; PreCG, Pre-Central insular Gyrus; SMA, Supplementary Motor Area; VMpo, Ventral Medial thalamic nucleus.

1. Introduction

Over the last two decades, a discrete number of brain regions have been shown to respond, more or less consistently, to painful sensations (Apkarian et al., 2005; Peyron et al., 2000; Tracey and Mantyh 2007), leading to the concept of pain matrix. These regions include cerebellum, putamen, thalamus, insular cortex (IC), anterior cingulate cortex (ACC), secondary somatosensory cortex (S2), primary somatosensory cortex (S1), supplementary motor area (SMA) and premotor area (Bornhövd et al., 2002; Büchel et al., 2002; Coghill et al., 1999), some of these brain areas being activated as a function of perceived pain (Büchel et al., 2002; Bornhövd et al., 2002; Oertel et al., 2011). Among this network, the operculo-insular and the anterior cingulate regions are considered as having the most consistent activations and as being of crucial importance for thermosensory and pain processing (Garcia-Larrea et al., 2010; Peyron et al., 2000; Tracey and Mantyh 2007).

However, within these regions, there are still major uncertainties on the temporal dynamics of pain responses responses, the approach of which is generally investigated with laser-evoked potentials (LEPs) and their low spatial resolution and their low brain sampling (Frot et al., 2007; Garcia-Larrea et al., 2010; Isnard et al., 2011). In a first attempt to answer this issue, Casey and colleagues (2001) defined early and late nociceptive responses with technical limitations due to the poor temporal resolution of positron emission tomography (PET). Thereafter, functional magnetic resonance imaging (fMRI) has improved a lot the temporal resolution, but only recently a few fMRI studies investigated these chronological aspects. They showed that blood-oxygen-level dependent (BOLD) responses within the pain matrix were not synchronous (Moulton et al., 2005) and that the shape of the BOLD response to pain was different of a canonical response (Chen et al., 2011; López-Solà et al., 2010; Upadhyay et al., 2010). In addition, within the pain matrix, the specificity of the activations for pain has been recently brought to controversy. It has been

proposed that sensorial visual and auditory processes could share with pain processes a common and unspecific pattern of activations (Mouraux and Iannetti 2009; Mouraux et al., 2011), considered as being related to the salience of stimuli (Baliki et al., 2009; Legrain et al., 2010).

In the present study, we concentrated on the operculo-insular and anterior cingulate cortices to investigate with optimized temporal resolution the shape and dynamics of the BOLD response to painful and non-painful events. To this aim, we exploited the finding that for a given intensity of laser stimulation, perception may be very different, the main advantage of such a dissociation between stimulus-intensity and pain perception being that the brain interprets as painful or not, stimulations of identical energy. Comparisons of BOLD responses to stimuli perceived as painful to those perceived as non-painful with two different methods provide the opportunity to directly assess specificities of pain responses.

2. Materials and Methods

2.1. Participants

Twenty-one healthy subjects participated in the study (10 females, 11 males; mean age: 24.9 years [SD 4.25]). Seventeen were right-handed according to the Edinburgh inventory (Oldfield et al., 1971). Participants had no history of neurological, psychiatric or chronic pain disease and did not take any medication except contraceptive. They were paid for their participation, and all provided written informed consent. The Ethics Committee of Saint-Etienne University Hospital, France approved the study.

2.2. Stimuli

Perception and nociceptive thresholds were determined the week before the fMRI session by delivering three consecutive stimuli at increasing and decreasing intensities. They were defined

as the lowest intensities at which the subjects considered at least 50 % of the stimuli as perceived or painful, respectively. Laser stimulations were applied with a Nd:YAP laser device ($\lambda = 1.34 \mu\text{m}$, duration: 5 ms, diameter: 6 mm, adapted to A δ fibers) on the radial dorsum of the left hand. Stimulation intensity was set to a subject's rating score of 4-5 on a 10-points pain scale. Laser spot was moved after each stimulation to prevent sensitization or habituation of skin receptors. To adjust the extremity of the laser fiber orthogonally to the skin and to ensure a constant distance to the skin, the extremity of the laser beam was fixed in a homemade support arm, allowing movements in the horizontal plane and preventing from movement of the experimenter. In this study, we used our experience and the observation that, for a given intensity of stimulation (low range of A δ fibers threshold), in the conditions described above, stimuli may be either perceived as painful or not painful.

2.3. Design

The paradigm was presented with E-Prime[®] 2.0 Professional presentation software (Psychology Software Tools Inc., www.pstnet.com, 2010) connected to a 1400 x 1050 pixels video projector positioned at the feet of the subject. Visual cue for rating was displayed on the projection screen with a 40 x 50 cm size and the subjects could see it by mean of mirrors positioned on the head coil.

A total of 184 laser stimulations were distributed over 4 different sessions of 46 stimulations. The length of each session was 12' 05". After each stimulation, when visual cue appeared in their visual field, subjects were asked to indicate whether the stimulation was painful (P) or non-painful (NP) by pressing a R/L button with the index and middle finger of the right hand. We preferred not to use a visual analog scale to score pain intensity during scanning to minimize the cognitive processing associated with the subject's response (Schoedel et al., 2008). In the absence of response, stimulus was considered as not felt. The delay between stimulation and

rating signal as well as the delay between rating signal and next stimulation were jittered to decorrelate and properly sample hemodynamic response of both types (mean: 2.9 s, range: 1.25 to 7.5 s and 11.7 s, range: 4.8 to 20 s respectively) according to Dale (Dale et al., 1999). The optseq software (<http://surfer.nmr.mgh.harvard.edu/optseq>, 2010) was used to generate four different timings of events, which were randomly presented to the subjects in four sessions.

2.4. Data acquisition

Blood oxygenation level dependent (BOLD) response was recorded on a 3T magnetic resonance scanner (Verio, Siemens) equipped with a 12-channel head coil. The subject's head was immobilized using foam pads. High-resolution (TR: 1800 ms, TE: 2.4 ms, 224 slices, voxel size: 0.9 x 0.9 x 0.9 mm) T1-weighted anatomical images were acquired in the sagittal plane for each subject. Using a T2*-weighted EPI (TR: 641 ms, TE: 30 ms, flip angle 90°, FoV = 224 mm, voxel size: 3.5 x 3.5 x 7 mm), 1123 imaging volumes per session were acquired. Gradient spoiling, consisting in 3 diffusion gradients in opposite phase, was used to reduce residual magnetization due to the short-TR acquisition. The sequence had three gradient spoilers to deal with carry-over effects due to the use of a short TR. The acquisition of 10 continuous slices (matrix = 64 x 64) was centered on the insula (orientation: AC-PC + 30°, figure 1). Primary sensory motor cortices as well as occipital cortices were therefore not scanned.

2.5. Preprocessing

fMRI data were preprocessed and analyzed with SPM8 (Wellcome Trust Centre for Neuroimaging). The first 7 functional scans from each session were discarded prior to the subsequent analyses. EPI images were realigned and averaged. Anatomical images were coregistered to the mean functional image and then they were passed through the 'segment' function which segments, bias corrects and spatially normalizes the data, all in the same model

(Ashburner and Friston 2005). The normalization parameters were then applied to the T1 and EPI images. EPI were resampled at 2 x 2 x 2 mm for the canonical and temporal derivative HRF analysis and at 4 x 4 x 4 mm for the finite impulse response analysis (see below). Then, both data sets were smoothed with a 7 x 7 x 7 mm full-width at half-maximum Gaussian kernel in order to reduce residual intersubject variability, which is about 5mm (Crinion et al., 2007). Normalized anatomical images of all subjects were averaged for subsequent localization of statistical results. High-pass filtering (cutoff period of 128 s) was applied to reduce the effect of slow signal drifts and the serial correlation was compensated by “prewhitening” the data with a first-order autoregressive model.

2.6. Preparation of the data for first-level analyses

Statistical analyses at the first level were calculated using an event-related design, with four types of events (P, NP, visual cue, rating) and four runs. Undetected stimuli were not modeled. Sessions comprising only P or only NP events were discarded from the analysis (1 session for 3 subjects). The six motion parameter vectors from the realignment procedure were included as regressors of no interest to account for artifacts caused by head motion.

2.7. Shape of BOLD: ‘FIR analysis’

In order to characterize the hemodynamic response (HR) to laser stimuli in regions known to respond to painful events, and thus to differentiate its shape according to the quality of the perception (P or NP), a finite impulse response (FIR) analysis was used to extract condition-specific HR time course, without *a priori* on its shape (Henson 2003). P and NP events were modeled with FIR while visual cue and motor response were modeled with canonical HRF. Time window was set to 25 s corresponding to the independent evaluation of the BOLD response in 39 time segments (called ‘time bins’) of 641 ms length each. This method also permitted to extract accurate latency (time-to-peak) values from the curves and to make good estimates of P vs. NP latency differences.

Amplitude and width that are not independent parameters (Lindquist and Wager 2007) were not estimated with FIR.

Subject-specific F-contrasts were computed to evaluate the entire time window in P and NP conditions. Then, we extracted HR of P and NP conditions from the first eigenvalue in 11 boxes covering the insula, on both sides. Since the effective resolution of our images is about 3.5 x 3.5 x 7 mm, boxes were defined as cubes 12 mm on a side. The first four boxes were positioned along the major anterior-posterior axis of the insula. Then other boxes were positioned above and below providing 11 boxes named according to their position: A1 to A3 in the anterior, M1 to M4 in the median and P1 to P4 in the posterior parts of the insula, with a -c suffix for the side contralateral to stimulation and a -i suffix for ipsilateral boxes. Voxels located outside the volume acquired in all subjects or outside the mean anatomical volume of the insula were excluded. Additionally, P and NP HRs were extracted in anterior midcingulate cortex (aMCC), defined as the intersection between acquisition volume common to all subjects and aMCC region. The subregions of the cingulate cortex were defined as the intersection between the cingulate cortex from AAL toolbox (Automatic Anatomical Labelling, Maldjian et al., 2003; Tzourio-Mazoyer et al., 2002) and the subregions from the Vogt nomenclature (Vogt et al., 2003; Vogt 2005).

2.8. Differences in amplitude of BOLD: 'HRF analysis'

In order to map condition-specific differences in amplitude of HRF, a more classical SPM analysis was done. The four event types were modeled using a canonical HRF and its time derivative to consider time variation in the HRF peak. This analysis will be called 'HRF analysis' in this paper. After computing subject-specific T-contrasts, a random-effects analysis across the group included all 21 subjects contrasts and was performed using one-sample t tests (Friston et al., 2005). Results are reported at a $p < 0.05$ family-wise error (FWE) corrected threshold, on the mean anatomical image.

2.9. Differences in latency of BOLD

Differences in latencies of BOLD responses were computed from both FIR and canonical and time derivative HRF analyses. Firstly, from curves estimated with the 'FIR analysis' for each participant and each condition, time-to-peak was measured. The peak was searched inside a time window from 3.5 s to 7 s in order to avoid physiologically implausible results (Calhoun et al., 2004; Steffener et al., 2010). Statistical significance of latency differences between conditions were conducted on R (<http://www.r-project.org>, 2010) with non-parametric paired Wilcoxon tests (df = 1) because of the ordinal class of the data. Spearman rho (ρ) was computed to test the correlation between anterior-posterior position and time-to-peak values. Results were reported significant at a $p < 0.05$ after false discovery rate (FDR) correction for multiple comparisons (n=484).

Secondly, using data of the 'HRF analysis', voxel-wise time-to-peak maps were built according to the method developed by Steffener (Steffener et al., 2010). It takes into account information from both canonical and temporal derivative HRFs to be specifically sensitive to temporal shifts. After computing single-subject time-to-peak images for both P and NP conditions, paired non-parametric tests (5000 permutations) were performed to compare P to NP at group level, using SnPM8. This led to group maps of significant P vs. NP latency differences. Results are reported at a $p < 0.05$ family-wise error (FWE) corrected threshold, on the mean anatomical image.

3. Results

3.1. Psychophysics

Laser stimulations were perceived as painful (P) in (mean [SD]) 52.7 % (20.3) of cases and as non-painful (NP) in 43.3 % (18.5) of cases. They were undetected in only 4 % (5.9) of cases. The proportions of NP and P stimuli did not differ across sessions (Friedman test, df = 3, NP: $\chi^2 = 2.99$,

$p = 0.39$; $P: \chi^2 = 3.34, p = 0.34$). Compared to undetected stimuli, both NP and P conditions were significantly more frequent (paired Wilcoxon tests on undetected vs. NP or P for each session: $p = 0.00094$ FDR). The proportion of NP stimuli was not different from those of P, across sessions (paired Wilcoxon tests on NP vs. P for each session: $p > 0.29$ FDR, figure 2a). Mean perceived intensity of painful stimuli was stable across sessions: 4.36 (1.66) (Friedman test, $df = 3, \chi^2 = 4.45, p = 0.22$, figure 2b).

3.2. Shape of BOLD

HR shape as estimated by the 'FIR analysis', for P and NP stimuli looks like a canonical HRF peaking around 5 s for all boxes studied (figure 3, figure 4).

3.3. Differences in amplitude of BOLD

Canonical HRF contrasts for P and NP stimulations activated brain regions of the pain matrix that were included in the acquisition volume, i.e. both ipsi- and contralateral anterior insular cortices (AIC), aMCC, S2, middle frontal cortex (Fmid), caudate nucleus, thalamus and cerebellum. Activations elicited by P stimuli as compared to NP stimuli were generally more extended, particularly in a posterior direction for the insular cortex (table 1 a & b).

Canonical P – NP contrast showed significant differences in the inferior middle and superior posterior insula bilaterally, in a small cluster in aMCC (figure 5, table 1c). According to the superimposition of P – NP contrast on the anatomical and functional subdivisions described in the operculo-insular cortices (Eickhoff et al., 2006b; Kurth et al., 2010a; Mazzola et al., 2012), P stimuli activated more intensely than NP the postcentral insular gyrus (PostCG), part of the granular insular cortex (Ig2) as well as medial parts of the parietal operculum (OP2, OP3). Unlike contralateral activation, the ipsilateral activation was extended anteriorly to the precentral (PreCG) and middle short (MSG) insular gyri.

3.4. Differences in latency of BOLD

In A1-c and A2-c as well as M3-i boxes, latencies extracted from 'FIR analysis' were significantly shorter in P as compared to NP conditions (A1-c: $p = 0.027$, A2-c: $p = 0.03$, M3-i: $p = 0.038$ FDR, figure 3). A2-i and A3-c boxes had a similar (sub-significant) trend to an earlier response in P compared to NP conditions (A2-i: $p = 0.056$, A3-c: $p = 0.054$ FDR, figure 3). There was a linear relationship between the position along the (y) anterior-posterior axis and latency, only in contralateral insula and only for painful conditions ($\rho = 0.87$, $p = 0.00046$, figure 6). There was no significant correlation in other conditions (table 2). There was no significant difference in time-to-peak between ipsi- and contralateral insula except in M1 which ipsilateral response peaked later than contralateral response both for painful and non-painful conditions (P: $p = 0.022$, NP: $p = 0.026$ FDR). In the contralateral aMCC, time-to-peak was significantly shortened in P as compared to NP conditions ($p = 0.016$ FDR, figure 4).

Accordingly, latency maps computed from 'HRF analysis' showed that only the anterior insular sulcus bilaterally (figure 7 a & b) and a small cluster of aMCC bilaterally (figure 7 c & d) responded more quickly during painful than during non-painful conditions.

4. Discussion

The present study investigated the localization and time dynamics of BOLD responses to a painful sensation, as compared to an identical stimulation that was perceived as non-painful. The two different methods that were used here to assess the BOLD response to pain ('FIR' and 'HRF' analyses) provided very consistent results. Within the investigated volume, they confirmed that the insular and anterior cingulate cortices were bilaterally involved in response to laser stimuli, in agreement with previous functional imaging studies (Apkarian et al., 2005; Peyron et al., 2000;

Tracey and Mantyh 2007), intra-cranial recordings (Frot et al., 2007) or stimulation studies (Mazzola et al., 2011).

This study demonstrates a specific association of painful sensations and increased amplitude of the BOLD response in the middle and posterior parts of the insular cortex. This regional distinction has been made possible by recent advances in the knowledge of the functional anatomy of the insular cortex showing different structural and functional role of several subdivisions (Eickhoff et al., 2006a; Brooks and Tracey 2007; Kurth et al., 2010b). In previous functional imaging studies, operculo-insular responses were often considered as a whole and this region was activated by various kinds of thermal stimuli, even at a non-noxious intensity of stimulation (Bornhövd et al., 2002; Büchel et al., 2002; Coghill et al., 1999; Craig et al., 2000). Thus, dissociating warm responses from pain responses in a brain region which anatomical subdivisions and specificities were not taken into account may have explained that, except in recent studies (Oertel et al., 2011), researchers have failed to identify specific brain regions responding to pain and rather identified non specific areas responding to multi-sensorial inputs or salience of the inputs (Legrain et al., 2010; Mouraux et al., 2011).

Considering the recent controversy brought by Iannetti and Mouraux (Iannetti and Mouraux 2010; Mouraux et al., 2011) arguing in favor of the absence of specific cortical areas, our data at least demonstrate the presence of specific areas activated by pain. These results are in agreement with a recent meta-analysis by Kurth (Kurth et al., 2010b) presenting the middle and posterior part of the insula as involved in sensorimotor processing whereas the anterior part of the insula is dedicated to the emotional and affective (cognitive) processing of pain (Eickhoff et al., 2006a; Mazzola et al., 2011). More precisely, our results fit those of Oertel (Oertel et al., 2011) showing that only a small part of the posterior insula is specifically involved in pain processing. The shift toward a slightly more posterior activation in our study could be attributed to the somatotopic

organization of the insula with the representation of the face that is anterior to those of the upper limb (Baumgärtner et al., 2010; Brooks and Tracey 2005; Mazzola et al., 2009).

With a functional imaging study centering acquisition on the main region of interest and using an optimized temporal resolution, the posterior-mid insula was identified as preferentially responding to pain. This amplitude difference between painful and non-painful conditions was not observed in the anterior insula, contrary to other studies using longer duration of thermal stimuli (Liang et al., 2011; Brinkmeyer et al., 2010; Mobascher et al., 2009, 2010). According to the theory of saliency and its encoding in the anterior insula (Legrain et al., 2010), the more the anterior insula is activated before the stimulation the more the nature of a stimulus will be interpreted as painful (Boly et al., 2007; Ploner et al., 2010; Wiech et al., 2010). This discrepancy between our results and those obtained with similar laser stimuli can be explained either by a difference in amplitude that is present in the anterior insula before the stimulation onset or because a standard analysis also includes responses with different latencies (see below). Alternatively, less restrictive thresholds than ours (uncorrected vs. FWE) can also account for discrepancies in the anterior insular responses.

Interestingly, specific activation for pain sensation to laser stimuli in the mid-posterior insula had a localization that was very consistent with other techniques used for investigation of pain in humans, namely, LEPs recorded with intra cerebral electrodes showing the encoding of the pain sensation (Frot et al., 2007), as well as a specific pain-evoked sensation after electrical stimulation of the brain (Mazzola et al., 2011). These data suggest that the insular cortex can respond both to P and NP stimuli in its anterior portion, (possibly with a cognitive, attentional, anticipatory or affective function), but that the middle and posterior subdivisions could distinguish between non-painful and painful sensations. These results, as others with intra-cranial LEPs or stimulation are in favor of a primary discriminative cortex for noxious events, in the middle and posterior part of the insula. If we consider the recent study of insular activations during thermal stimulations (Mazzola

et al., 2012) and if there is one insular sub-division subserving pain-specific sensations, regardless the intensity of the physical stimulus, then Ig2 is the best candidate to mediate such specific pain processes. Accordingly, the neighboring Ig1 subdivision is the region that receives specific nociceptive afferences from the posterior part of the ventral medial thalamic nucleus (VMpo, Craig and Zhang 2006).

Comparatively to the results of standard fMRI analyses that we and others have reported in pain conditions, the FIR analysis allowed to extract a temporally well sampled insular HR. Unlike previous studies of BOLD response to painful stimuli (Chen et al., 2011; López-Solà et al., 2010; Upadhyay et al., 2010), the HR shape in the insula was found to be similar to a canonical HR shape. This difference of results could be explained either by a difference in duration of stimuli (several seconds versus 5 ms) since long duration is not optimal for the analysis of single (event-related) response, or by a difference in temporal sampling. By reducing the duration of the recording for one brain volume to approximately 600 ms, one may expect to specify the temporal dynamics of the BOLD responses within the pain matrix. This challenge has been initiated in early PET studies by Casey (Casey et al., 2001) but it could not be extended more in details because of the poor temporal resolution of the PET. Nevertheless, these authors dissociated two kinds of responses (early and late) and others also succeeded in demonstrating that not all responses of the pain matrix occurred at the same time (Moulton et al., 2005).

Latency differences observed in this study are original observations that reminds of what we know from neurophysiological recordings on the temporal dynamics of brain responses. Such investigations could not be made with standard fMRI analyses because of the temporal resolution of acquisitions. For the first time, we illustrate that the anterior part of the insula responds earlier in painful than in non-painful conditions. It means that the anterior insula, that is known to code emotion and affect of pain, is treating faster nociceptive than non-nociceptive information. Recently, it was reported that differences in neural activation could result in changes in the

amplitude, in the latency, or in both amplitude and latency of the HR (Henson et al., 2002). The present study reports pure differences either in amplitude or in latency. In other words, posterior insular responses differ in terms of amplitude only while anterior insular responses differ in terms of latency only. In the field of somatosensory and pain responses, it has been reported that the time course of the response could be different and have a biphasic shape for heat pain as compared to brush (Upadhyay et al., 2010), and therefore, the amplitude, the shape, but also the latency of BOLD responses to stimuli may have an importance in how the brain interprets the inputs, including the nociceptive ones. In the present study, with two different methods providing very consistent results, we observed two time-dissociations, one in AIC as compared to PIC for painful stimuli only, and the other between contralateral (right) and ipsilateral (left) ICs. After a noxious laser input, the BOLD response is dissociated in time since it peaks earlier than for an innocuous laser input in the AIC. If we consider that the BOLD response in the mid and posterior insular cortex is determinant to define the painful nature of stimuli (through a coding of amplitude), then we have also to consider that when it is interpreted as painful, stimuli-evoked BOLD responses have a shortened latency in the anterior insular cortex. Larger amplitude of the response in the posterior insula may condition the velocity of the propagation to the anterior insula because of a potentially threatening or dangerous nature. In other words, there is an area (mid-posterior insula) responding first, this area is able to treat specifically painful information, and the information of how fast is the signal transmitted to another area (anterior insula) is meaningful regarding the anterior insular response supposed to mediate an on-time affective or emotional reaction. This view is supported by the correlation between the anterior-posterior position within the IC and the latency of response. Differences in vasculature can influence BOLD response that is known to be variable across brain regions (Aguirre et al., 1998; Handwerker et al., 2004) and the insular cortex is close to large blood vessels (Afif and Mertens 2010; Türe et al., 2000). However, such a vascular explanation does not apply to our results since the differences

reported here were relative to conditions (*i.e.* P or NP stimuli) and concerned the same regions. Similarly, differences of latencies between contralateral (early) and ipsilateral (late) insula responses (M1 box) may not be explained by differences in vasculature, but rather by temporal dynamics of the response, in agreement with what is known from neurophysiological response firstly contralateral to stimulation and secondly ipsilateral with a callosal transfer of 15 ms (Frot and Mauguière 2003).

Because of possible differences in vasculature, latencies in aMCC cannot be directly compared to the BOLD response in the insula, even though the latency is superior to 5 s in aMCC and inferior to 5 s in posterior insula. However, the differences between P and NP conditions suggests, as for AIC, that the 'analytic' response in posterior/mid insular cortex can generate a BOLD response propagated more or less rapidly to other areas of the pain matrix, particularly in the medial pain system (AIC and aMCC), the processing being able to alert more rapidly these regions if stimuli represent a threat for the subject.

As a perspective it would be interesting to study effective connectivity, for example with DCM, to confirm or not the sequential activation of the different parts of the insular and cingulate cortices. The double dissociation between i/ amplitude and latencies of the responses and ii/ subdivisions of insular cortex should prompt fMRI investigations taking into account these specificities of BOLD responses in other parts of the pain matrix.

5. Conclusions

BOLD responses to painful laser stimuli were differentiated from those to non-painful laser stimulation. The posterior and middle parts of the insula respond more intensively to pain, while the anterior parts respond faster. There is a dissociation between latency coding and intensity coding for painful message in the anterior and posterior parts of the insula. This dissociation was not found in the anterior middle cingulate cortex that shows a hemodynamic

response to pain with both a greater intensity and a shorter latency than the hemodynamic response to a non-painful stimulation.

Acknowledgements

This work was supported by a grant from Institut UPSA de la douleur (appel d'offre 1998-1999) and Institut de France - Fondation NRJ 2010. We wish to thank Alice de Fréminville (Martin) for preliminary pilot studies on this project.

References

- Afif A, Mertens P. 2010. Description of sulcal organization of the insular cortex. *Surg Radiol Anat.* 32:491-498.
- Aguirre G, Zarahn E, D'esposito M. 1998. The variability of human, BOLD hemodynamic responses. *NeuroImage.* 8:360-369.
- Apkarian A, Bushnell M, Treede R-D, Zubieta J-K. 2005. Human brain mechanisms of pain perception and regulation in health and disease. *Eur J Pain.* 9:463-484.
- Ashburner J, Friston KJ. 2005. Unified segmentation. *NeuroImage,* 26:839–851. doi:10.1016/j.neuroimage.2005.02.018
- Büchel C, Bornhövd K, Quante M, Glauche V, Bromm B, Weiller C. 2002. Dissociable neural responses related to pain intensity, stimulus intensity, and stimulus awareness within the anterior cingulate cortex: a parametric single-trial laser functional magnetic resonance imaging study. *J Neurosci.* 22:970-976.
- Baliki M, Geha P, Apkarian A. 2009. Parsing pain perception between nociceptive representation and magnitude estimation. *J Neurophysiol.* 101:875-887.
- Baumgärtner U, Iannetti G, Zambreanu L, Stoeter P, Treede R-D, Tracey I. 2010. Multiple somatotopic representations of heat and mechanical pain in the operculo-insular cortex: a high-resolution fMRI study. *J Neurophysiol.* 104:2863-2872.
- Boly M, Balteau E, Schnakers C, Degueldre C, Moonen G, Luxen A, Phillips C, et al., 2007. Baseline brain activity fluctuations predict somatosensory perception in humans. *PNAS,* 104:12187–12192.
- Bornhövd K, Quante M, Glauche V, Bromm B, Weiller C, Büchel C. 2002. Painful stimuli evoke different stimulus-response functions in the amygdala, prefrontal, insula and somatosensory cortex: a single-trial fMRI study. *Brain.* 125:1326-1336.

- Brinkmeyer J, Mobascher A, Warbrick T, Musso F, Wittsack H-J, Saleh A, Schnitzler A, et al., 2010. Dynamic EEG-informed fMRI modeling of the pain matrix using 20-ms root mean square segments. *Hum Brain Map*, 31:1702–1712.
- Brooks J, Tracey I. 2005. From nociception to pain perception: imaging the spinal and supraspinal pathways. *J Anat*. 207:19-33.
- Brooks J, Tracey I. 2007. The insula: a multidimensional integration site for pain. *Pain*. 128:1-2.
- Calhoun V, Stevens M, Pearlson G, Kiehl K. 2004. fMRI analysis with the general linear model: removal of latency-induced amplitude bias by incorporation of hemodynamic derivative terms. *NeuroImage*. 22:252-257.
- Casey KL, Morrow TJ, Lorenz J, Minoshima S. 2001. Temporal and spatial dynamics of human forebrain activity during heat pain: analysis by positron emission tomography. *J Neurophysiol*. 85:951-959.
- Chen L, Dillenburger B, Wang F, Friedman R, Avison M. 2011. High-resolution functional magnetic resonance imaging mapping of noxious heat and tactile activations along the central sulcus in New World monkeys. *Pain*. 152:522-532.
- Coghill R, Sang C, Maisog J, Iadarola M. 1999. Pain intensity processing within the human brain: a bilateral, distributed mechanism. *J Neurophysiol*. 82:1934-1943.
- Craig AD, Chen K, Bandy D, Reiman EM. 2000. Thermosensory activation of insular cortex. *Nat Neurosci*. 3:184-190.
- Craig A, Zhang E-T. 2006. Retrograde analyses of spinothalamic projections in the macaque monkey: input to posterolateral thalamus. *J Comp Neurol*. 499:953-964.
- Crinion J, Ashburner J, Leff A, Brett M, Price C, Friston K. 2007. Spatial normalization of lesioned brains: performance evaluation and impact on fMRI analyses. *NeuroImage*, 37:866–875.
- Dale A. 1999. Optimal experimental design for event-related fMRI. *Hum Brain Mapp*. 8:109-114.

- Eickhoff S, Amunts K, Mohlberg H, Zilles K. 2006a. The human parietal operculum. II. Stereotaxic maps and correlation with functional imaging results. *Cereb Cortex*. 16:268-279.
- Eickhoff S, Schleicher A, Zilles K, Amunts K. 2006b. The human parietal operculum. I. Cytoarchitectonic mapping of subdivisions. *Cereb Cortex*. 16:254-267.
- Friston K, Stephan K, Lund T, Morcom A, Kiebel S. 2005. Mixed-effects and fMRI studies. *NeuroImage*. 24:244-252.
- Frot M, Mauguière F. 2003. Dual representation of pain in the operculo-insular cortex in humans. *Brain*. 126:438-450.
- Frot M, Magnin M, Mauguière F, Garcia-Larrea L. 2007. Human SII and posterior insula differently encode thermal laser stimuli. *Cereb Cortex*. 17:610-620.
- Garcia-Larrea L, Perchet C, Creac'h C, Convers P, Peyron R, Laurent B, Mauguière F, Magnin M. 2010. Operculo-insular pain (parasyllian pain): a distinct central pain syndrome. *Brain*. 133:2528-2539.
- Handwerker D, Ollinger J, D'Esposito M. 2004. Variation of BOLD hemodynamic responses across subjects and brain regions and their effects on statistical analyses. *NeuroImage*. 21:1639-1651.
- Henson R, Price C, Rugg M, Turner R, Friston K. 2002. Detecting latency differences in event-related BOLD responses: application to words versus nonwords and initial versus repeated face presentations. *NeuroImage*. 15:83-97.
- Henson R. 2003. Analysis of fMRI time series: Linear time-invariant models, event-related fMRI, and optimal experimental design. In: Frackowiack R, *Human Brain Function 2nd ed.* San Diego (CA): Elsevier. pp793-823.
- Iannetti GD, Mouraux A. 2010. From the neuromatrix to the pain matrix (and back). *Exp Brain Res*, 205:1–12.

- Isnard J, Magnin M, Jung J, Mauguière F, Garcia-Larrea L. 2011. Does the insula tell our brain that we are in pain? *Pain*. 152:946-951.
- Kurth F, Eickhoff S, Schleicher A, Hoemke L, Zilles K, Amunts K. 2010a. Cytoarchitecture and probabilistic maps of the human posterior insular cortex. *Cereb Cortex*. 20:1448-1461.
- Kurth F, Zilles K, Fox P, Laird A, Eickhoff S. 2010b. A link between the systems: functional differentiation and integration within the human insula revealed by meta-analysis. *Brain Struct Funct*. 214:519-534.
- Legrain V, Iannetti G, Plaghki L, Mouraux A. 2010. The pain matrix reloaded A salience detection system for the body. *Prog Neurobiol*. 93:111-124.
- Liang M, Mouraux A, Iannetti GD. 2011. Parallel Processing of Nociceptive and Non-nociceptive Somatosensory Information in the Human Primary and Secondary Somatosensory Cortices: Evidence from Dynamic Causal Modeling of Functional Magnetic Resonance Imaging Data. *J Neurosci*, 31:8976–8985.
- Lindquist M, Wager T. 2007. Validity and power in hemodynamic response modeling: a comparison study and a new approach. *Hum Brain Mapp*. 28:764-784.
- López-Solà M, Pujol J, Hernández-Ribas R, Harrison B, Ortiz H, Soriano-Mas C, Deus J, Menchon JM, Vallejo J, Cardoner N. 2010. Dynamic assessment of the right lateral frontal cortex response to painful stimulation. *NeuroImage*. 50:1177-1187.
- Maldjian JA, Laurienti PJ, Kraft RA, Burdette JH. 2003. An automated method for neuroanatomic and cytoarchitectonic atlas-based interrogation of fMRI data sets. *NeuroImage*. 19:1233-1239.
- Mazzola L, Isnard J, Peyron R, Guénot M, Mauguière F. 2009. Somatotopic organization of pain responses to direct electrical stimulation of the human insular cortex. *Pain*. 146:99-104.

- Mazzola L, Isnard J, Peyron R, Mauguière F. 2011. Stimulation of the human cortex and the experience of pain: Wilder Penfield's observations revisited. *Brain*. 1–10. doi:10.1093/brain/awr265
- Mazzola L, Faillenot I, Barral FG, Mauguière F, Peyron R. 2012. Spatial segregation of somatosensory and pain activations in the human operculo-insular cortex. *NeuroImage*. 60:409–418.
- Mobascher A, Brinkmeyer J, Warbrick T, Musso F, Wittsack HJ, Saleh A, Schnitzler A, et al., 2009. Laser-evoked potential P2 single-trial amplitudes covary with the fMRI BOLD response in the medial pain system and interconnected subcortical structures. *NeuroImage*, 45:917–926.
- Mobascher A, Brinkmeyer J, Warbrick T, Musso F, Schlemper V, Wittsack HJ, Saleh A, et al., 2010. Brain activation patterns underlying fast habituation to painful laser stimuli. *International journal of psychophysiology*, 75:16–24.
- Moulton E, Keaser M, Gullapalli R, Greenspan J. 2005. Regional intensive and temporal patterns of functional MRI activation distinguishing noxious and innocuous contact heat. *J Neurophysiol*. 93:2183-2193.
- Mouraux A, Iannetti G. 2009. Nociceptive laser-evoked brain potentials do not reflect nociceptive-specific neural activity. *J Neurophysiol*. 101:3258-3269.
- Mouraux A, Diukova A, Lee M, Wise R, Iannetti G. 2011. A multisensory investigation of the functional significance of the 'pain matrix'. *NeuroImage*. 54:2237-2249.
- Oertel BG, Preibisch C, Martin T, Walter C, Gamer M, Deichmann R, Lötsch J. 2011. Separating brain processing of pain from that of stimulus intensity. *Hum Brain Mapp*. doi:10.1002/hbm.21256
- Oldfield R. 1971. The assessment and analysis of handedness: the Edinburgh inventory. *Neuropsychologia*. 9:97-113.
- Optseq Software, <http://surfer.nmr.mgh.harvard.edu/optseq>, 2010.

- Peyron R, Laurent B, García-Larrea L. 2000. Functional imaging of brain responses to pain. A review and meta-analysis (2000). *Clin Neurophysiol.* 30:263-288.
- Ploner M, Lee MC, Wiech K, Bingel U, Tracey I. 2010. Prestimulus functional connectivity determines pain perception in humans. *PNAS.* 107:355–360.
- Psychology Software Tools, www.pstnet.com, 2010.
- R Software, <http://www.r-project.org>, 2010.
- Schoedel A, Zimmermann K, Handwerker H, Forster C. 2008. The influence of simultaneous ratings on cortical BOLD effects during painful and non-painful stimulation. *Pain.* 135:131-141.
- Steffener J, Tabert M, Reuben A, Stern Y. 2010. Investigating hemodynamic response variability at the group level using basis functions. *NeuroImage.* 49:2113-2122.
- Tracey I, Mantyh PW. 2007. The cerebral signature for pain perception and its modulation. *Neuron.* 55:377-391.
- Türe U, Yasargil MG, Al-Mefty O, Yasargil DC. 2000. Arteries of the insula. *J Neurosurg.* 92:676-687.
- Tzourio-Mazoyer N, Landeau B, Papathanassiou D, Crivello F, Etard O, Delcroix N, Mazoyer B, Joliot M. 2002. Automated anatomical labeling of activations in SPM using a macroscopic anatomical parcellation of the MNI MRI single-subject brain. *NeuroImage.* 15:273-289.
- Upadhyay J, Pendse G, Anderson J, Schwarz A, Baumgartner R, Coimbra A, Bishop J, Knudsen J, George E, Grachev I, Iyengar S, Bleakman D, Hargreaves R, Borsook D, Becerra L. 2010. Improved characterization of BOLD responses for evoked sensory stimuli. *NeuroImage.* 49:2275-2286.
- Vogt BA, Berger GR, Derbyshire SW. 2003. Structural and functional dichotomy of human midcingulate cortex. *Eur J Neurosci.* 18:3134-3144.
- Vogt BA. 2005. Pain and emotion interactions in subregions of the cingulate gyrus. *Nat Rev Neurosci.* 6:533-544.

Wiech K, Lin C-S, Brodersen K H, Bingel U, Ploner M, Tracey I. 2010). Anterior insula integrates information about salience into perceptual decisions about pain. *J Neurosci*, 30:16324–16331.

Captions

Figure 1

Acquisition field of one representative subject.

10 contiguous slices, 7 mm thick were acquired in AC-PC + 30° plane, centered on the insular cortex.

Figure 2

Psychophysical results.

(a) Percentage of painful (P), non-painful (NP) and undetected laser stimulations per session in chronological order represented as mean \pm SD of 21 subjects. The proportion of P and NP sensations evoked by laser stimuli was equivalent. For the intensities of stimulation that were used, the percentage of undetected stimuli was rare and differed significantly from the percentage of perceived (painful or not) stimuli. The order of the four different sessions was randomized across subjects. Trends to sensitization for P conditions and to habituation for NP conditions across sessions were not significant. Proportions of NP and P stimuli were not different, whatever the session. (b) Mean pain rating \pm SD for painful condition recorded at the end of each session. Please note that sessions did not statistically differ in terms of pain intensity.

Figure 3

Shape and differences in latency of BOLD response in the insula.

Hemodynamic responses extracted from 'FIR analysis' (finite impulse response), without a priori information on latency. Mean \pm SEM was calculated from subject-specific eigenvalue of 11 boxes (33 voxels) on both (a) contralateral and (b) ipsilateral insula. Time course of the hemodynamic response is represented as percent of signal change on a 25 s time window starting at the onset of

laser stimuli, with a temporal resolution of 641 ms. Significant differences of latency between painful and non-painful conditions are represented (Paired Wilcoxon tests, ** $p < 0.05$, * $p < 0.1$ FDR corrected). There was no time-to-peak difference between ipsi- and contralateral insula except in M1 box: M1-c response peaking before M1-i response for both painful and non-painful conditions (paired Wilcoxon tests, $p < 0.05$ FDR corrected). Please note that M2-M4 and P1 boxes displayed differences of amplitude in BOLD response as shown in figure 5.

Figure 4

Shape and differences in latency of BOLD response in aMCC.

Hemodynamic responses extracted from 'FIR analysis' (finite impulse response), without *a priori* information on latency. Mean \pm SEM was calculated from subject-specific eigenvalue of anterior midcingulate cortex (aMCC) on both (a) contralateral and (b) ipsilateral side. Time course of the hemodynamic response is represented as percent of signal change on a 25 s time window starting at the onset of laser stimuli. The hemodynamic response to painful condition peaks significantly earlier than the response to non-painful condition in the contralateral aMCC (Paired Wilcoxon tests, ** $p < 0.05$ FDR corrected).

Figure 5

Differences in amplitude of BOLD responses.

Activation maps of painful – non-painful (canonical HRF) contrast from group random-effects 'HRF analysis' ($p < 0.05$ FWE corrected) superimposed on the 11 boxes for (a) contralateral and (b) ipsilateral insula (voxel size: 4 x 4 x 4 mm); and superimposed on anatomical (c) anterior midcingulate cortex (aMCC, voxel size: 2 x 2 x 2 mm). Please note that in the insula, the only subdivisions to be more activated in painful than in non-painful condition are the posterior and the mid parts bilaterally.

Figure 6

Correlation between latencies and anterior-posterior position.

Median latency (time-to-peak) in seconds in contralateral insula for painful condition, represented as a function of y-axis in MNI coordinates (negative value: posterior, positive value: anterior). Only contralateral insula showed a significant correlation between latency and Y coordinates at $p < 0.05$ (Spearman correlation test, $\rho = 0.87$, $p = 0.00046$). In other words, the hemodynamic response to painful stimuli peaks earlier in the posterior insula than in the anterior insula on the side contralateral to laser stimulation.

Figure 7

Map of latency differences.

Map of latency differences between non-painful and painful conditions for the group (latencies for painful conditions are shorter than for non-painful conditions) superimposed on the 11 boxes in (a) contralateral, (b) ipsilateral insula, (c) contralateral and (d) ipsilateral anterior midcingulate cortex (aMCC). Please note that only the anterior part of the insula as well as a small cluster in aMCC are concerned by this latency difference (non-parametric tests on individual voxel-wise time-to-peak maps, $p < 0.05$ FWE, Steffener et al., 2010).

Tables

Table 1

Coordinates in MNI space of activation peaks for canonical HRF.

(a) Non-painful contrast, (b) painful contrast, (c) painful – non-painful contrast from group random-effects analysis ($p < 0.05$ FWE corrected at voxel level). T score and P value of the voxel corresponding to the peak of clusters; voxels represents number of voxels in the cluster. aMCC: anterior midcingulate cortex, S2: secondary somatosensory cortex, DLPF: dorsolateral prefrontal cortex, I: ipsilateral (left), C: contralateral (right).

Table 2

Median latencies in seconds.

Median latency of activation (in seconds) for each subdivision of the ipsilateral and contralateral insula in both painful and non-painful conditions, obtained with 'FIR analysis'.

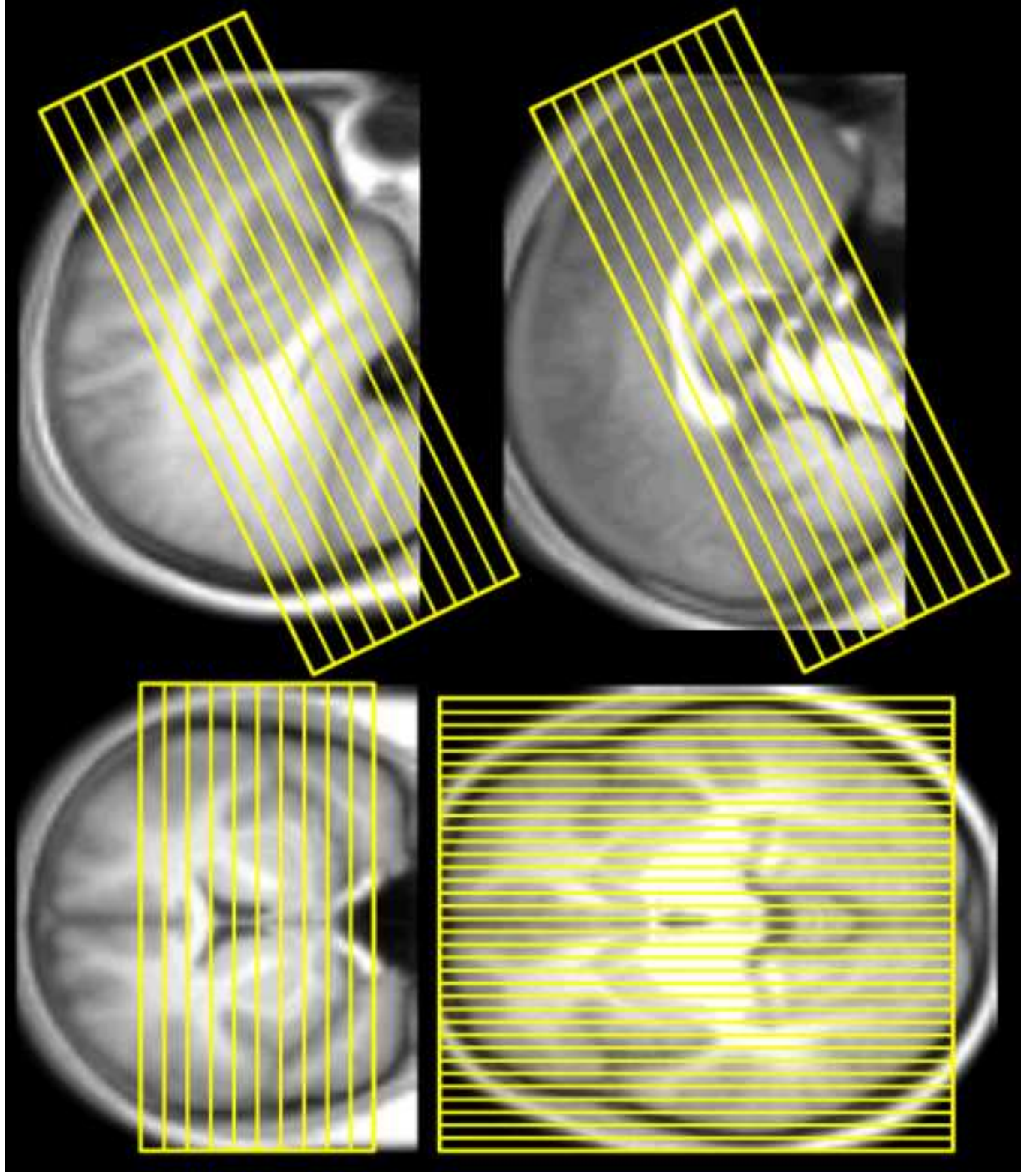
8. Table 1

| Region | Side | a. Non-painful | | | | | | b. Painful | | | | | | c. Painful - Non-Painful | | | | | |
|--------------------|------|----------------|-----|-----|-------------|---------|--------|-------------|-----|------|-------------|---------|--------|--------------------------|-----|------|-------------|---------|--------|
| | | Coordinates | | | Voxel level | | | Coordinates | | | Voxel level | | | Coordinates | | | Voxel level | | |
| | | X | Y | Z | T score | P value | Voxels | X | Y | Z | T score | P value | Voxels | X | Y | Z | T score | P value | Voxels |
| Anterior insula | I | -38 | 14 | -2 | 11.85 | 0.000 | 3325 | -36 | 14 | -4 | 20.28 | 0.000 | 9493 | | | | | | |
| | C | -32 | 20 | -4 | 11.51 | 0.001 | | -28 | 16 | 0 | 17.94 | 0.000 | | | | | | | |
| | C | 34 | 14 | 2 | 11.88 | 0.000 | | 38 | 18 | -4 | 18.03 | 0.000 | | | | | | | |
| | | 38 | 0 | -8 | 6.09 | 0.038 | 5 | | | | | | | | | | | | |
| aMCC | I | -6 | 20 | 34 | 10.86 | 0.000 | 1265 | -2 | 28 | 28 | 14.95 | 0.000 | 2327 | | | | | | |
| | C | 6 | 22 | 32 | 11.22 | 0.000 | | -8 | 16 | 34 | 13.24 | 0.000 | | | | | | | |
| | | | | | | | | 2 | -22 | 34 | 14.21 | 0.000 | | | | | | | |
| Posterior insula | I | -38 | -4 | 16 | 10.25 | 0.000 | 99 | -38 | -2 | 14 | 13.26 | 0.000 | 9493 | -38 | -12 | 4 | 8.52 | 0.001 | 495 |
| | C | -36 | -4 | -8 | 6.43 | 0.022 | 15 | -38 | -14 | 16 | 6.61 | 0.015 | 9493 | -38 | -18 | 14 | 8.23 | 0.001 | |
| | C | 38 | -4 | -10 | 5.93 | 0.050 | 1 | 40 | -14 | 16 | 6.91 | 0.009 | 9493 | -34 | 6 | 10 | 8.09 | 0.002 | |
| | | | | | | | 40 | 0 | 8 | 8.89 | 0.000 | 9493 | 42 | -12 | 12 | 8.84 | 0.001 | 315 | |
| | | | | | | | | | | | | | 38 | -6 | -6 | 7.89 | 0.002 | | |
| | | | | | | | | | | | | | 40 | -10 | 2 | 7.31 | 0.006 | | |
| DLPF | I | -34 | 48 | 10 | 6.60 | 0.016 | 69 | -30 | 44 | 18 | 8.15 | 0.001 | 493 | | | | | | |
| | C | -30 | 42 | 20 | 6.52 | 0.018 | | -36 | 46 | 10 | 7.48 | 0.004 | | | | | | | |
| | C | 38 | 42 | 4 | 6.39 | 0.023 | 7 | -34 | 32 | 22 | 7.15 | 0.006 | 34 | | | | | | |
| | | | | | | | 40 | 38 | 12 | 6.45 | 0.020 | | | | | | | | |
| | | | | | | | 38 | 40 | 4 | 6.43 | 0.020 | | | | | | | | |
| Frontal inferior | I | -56 | 6 | 10 | 9.13 | 0.000 | 193 | -54 | 6 | 12 | 6.13 | 0.000 | 9493 | | | | | | |
| | C | -34 | 30 | 24 | 6.27 | 0.028 | 4 | | | | | | | | | | | | |
| | C | -10 | -76 | -42 | 5.95 | 0.048 | 1 | | | | | | | | | | | | |
| Cerebellum | I | | | | | | | -30 | -56 | -30 | 7.45 | 0.004 | 138 | | | | | | |
| | C | | | | | | | -22 | -60 | -34 | 6.01 | 0.041 | | | | | | | |
| | C | | | | | | | -10 | -74 | -42 | 6.94 | 0.009 | 100 | | | | | | |
| | | | | | | | -8 | -74 | -24 | 6.85 | 0.010 | | | | | | | | |
| | | | | | | | -14 | -66 | -28 | 6.10 | 0.036 | | | | | | | | |
| | | | | | | | 34 | -54 | -28 | 8.51 | 0.001 | 610 | | | | | | | |
| | | | | | | | 16 | -54 | -20 | 7.93 | 0.002 | | | | | | | | |
| | | | | | | | 26 | -52 | -24 | 7.32 | 0.005 | | | | | | | | |
| | | | | | | | 24 | -70 | -18 | 6.00 | 0.042 | 5 | | | | | | | |
| S2 | I | -58 | -20 | 18 | 8.63 | 0.001 | 58 | -58 | -18 | 18 | 10.34 | 0.000 | 9493 | | | | | | |
| | C | 56 | -16 | 18 | 8.59 | 0.001 | 52 | 58 | -14 | 18 | 9.43 | 0.000 | 9493 | | | | | | |
| | C | -40 | -50 | 6 | 7.51 | 0.004 | 13 | -46 | -50 | 4 | 7.19 | 0.006 | 30 | | | | | | |
| | | | | | | | 58 | -42 | 10 | 6.31 | 0.025 | 3 | | | | | | | |
| Hippocampus | I | | | | | | | -18 | -38 | 0 | 6.73 | 0.012 | 24 | | | | | | |
| | C | | | | | | | 0 | -52 | -30 | 6.88 | 0.009 | 22 | | | | | | |
| | C | | | | | | | 6 | -64 | -14 | 5.94 | 0.046 | 1 | | | | | | |
| | | | | | | | | 44 | -24 | -6 | 6.27 | 0.027 | 10 | | | | | | |
| Temporal superior | C | 12 | -6 | 0 | 5.97 | 0.047 | 1 | -4 | -12 | 0 | 10.51 | 0.000 | 9493 | 6 | -26 | -8 | 6.66 | 0.017 | 9 |
| | C | | | | | | | | | | | | | | | | | | |
| | C | | | | | | | | | | | | | | | | | | |
| Subthalamus | I | | | | | | | | | | | | | | | | | | |
| | C | | | | | | | | | | | | | | | | | | |
| | C | | | | | | | | | | | | | | | | | | |
| Frontal sup medial | I | | | | | | | | | | | | | | | | | | |
| | C | | | | | | | | | | | | | | | | | | |
| | C | | | | | | | | | | | | | | | | | | |
| Premotor | I | -40 | 0 | 28 | 6.16 | 0.034 | 3 | | | | | | | | | | | | |
| | C | | | | | | | | | | | | | | | | | | |
| | C | | | | | | | | | | | | | | | | | | |
| Amygdala | I | | | | | | | | | | | | | | | | | | |
| | C | | | | | | | | | | | | | | | | | | |
| | C | | | | | | | | | | | | | | | | | | |
| Temporal superior | I | | | | | | | | | | | | | | | | | | |
| | C | | | | | | | | | | | | | | | | | | |
| | C | | | | | | | | | | | | | | | | | | |

8. Table 2

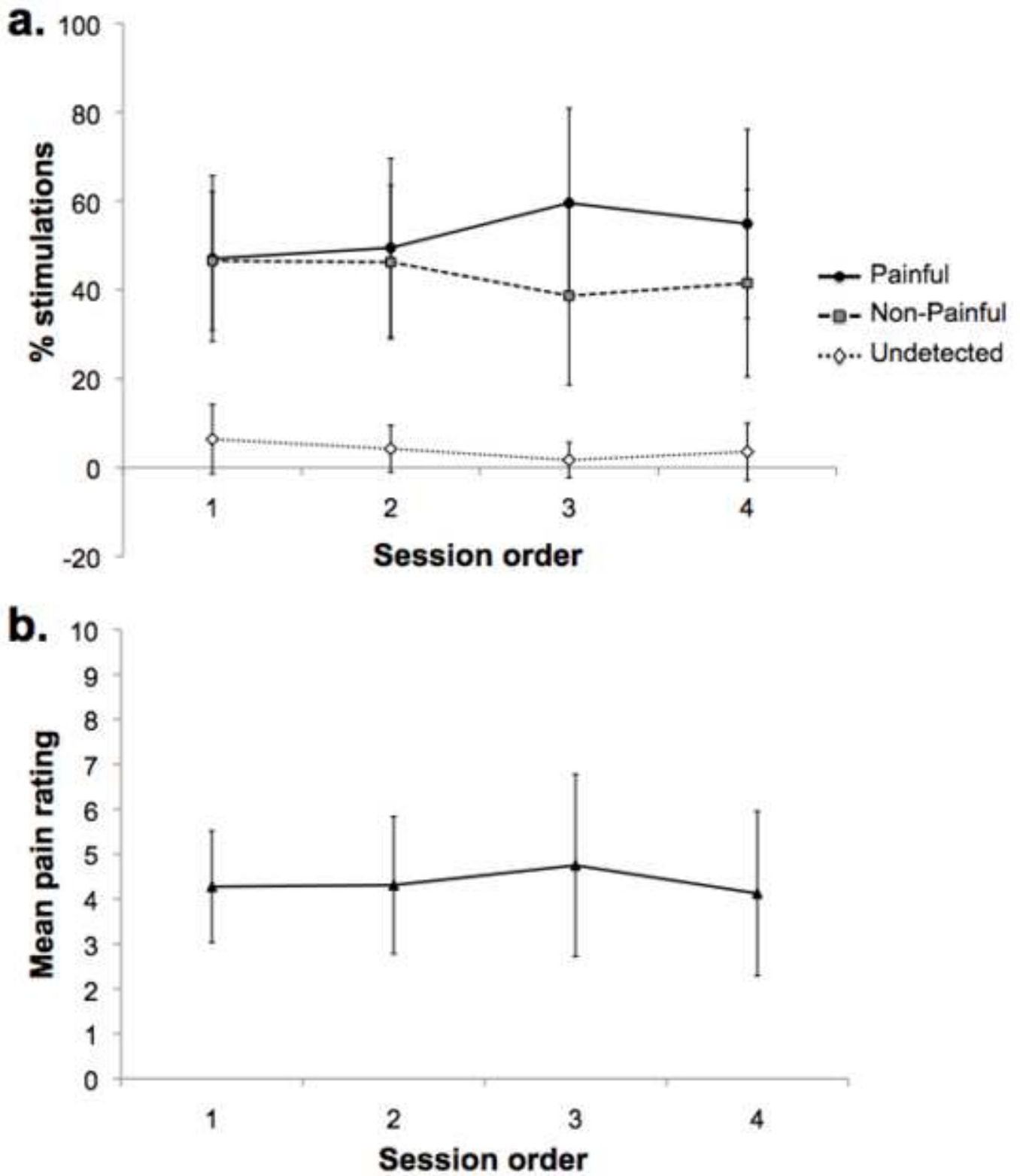
| | Ipsilateral | | | | | | Contralateral | | | | | |
|-----------|-------------|------|-------|---------|------|-------|---------------|------|-------|---------|------|-------|
| | Non-Painful | | | Painful | | | Non-Painful | | | Painful | | |
| | median | min | max | median | min | max | median | min | max | median | min | max |
| A1 | 5.45 | 3.53 | 9.94 | 5.45 | 0.32 | 11.22 | 5.45 | 4.17 | 6.73 | 5.45 | 4.17 | 6.73 |
| A2 | 6.09 | 4.81 | 7.37 | 5.45 | 4.17 | 6.73 | 4.17 | 0.32 | 9.94 | 4.81 | 4.17 | 10.58 |
| A3 | 5.45 | 4.17 | 7.37 | 4.81 | 4.17 | 6.73 | 2.88 | 0.32 | 8.01 | 4.81 | 4.17 | 6.73 |
| M1 | 4.81 | 2.24 | 8.01 | 5.45 | 4.17 | 9.29 | 4.81 | 3.53 | 6.73 | 4.81 | 4.17 | 6.73 |
| M2 | 4.81 | 3.53 | 6.73 | 4.81 | 4.17 | 6.73 | 5.45 | 2.88 | 12.50 | 4.81 | 2.88 | 5.45 |
| M3 | 5.45 | 0.32 | 6.73 | 4.81 | 3.53 | 5.45 | 4.17 | 0.96 | 8.65 | 4.81 | 3.53 | 5.45 |
| M4 | 4.17 | 0.32 | 12.50 | 4.81 | 2.24 | 5.45 | 4.17 | 0.32 | 9.94 | 4.81 | 3.53 | 6.73 |
| P1 | 5.45 | 1.60 | 6.73 | 4.81 | 3.53 | 12.50 | 5.45 | 3.53 | 6.73 | 4.17 | 2.24 | 12.50 |
| P2 | 6.09 | 2.24 | 11.22 | 5.45 | 3.53 | 11.86 | 5.45 | 3.53 | 8.01 | 4.17 | 0.96 | 12.50 |
| P3 | 4.17 | 0.96 | 6.73 | 4.17 | 2.88 | 9.29 | 4.17 | 0.32 | 6.73 | 4.17 | 0.96 | 6.09 |
| P4 | 4.81 | 0.32 | 8.65 | 4.17 | 0.96 | 9.29 | 6.09 | 3.53 | 7.37 | 4.17 | 0.32 | 5.45 |

9. Figure 1
[Click here to download high resolution image](#)

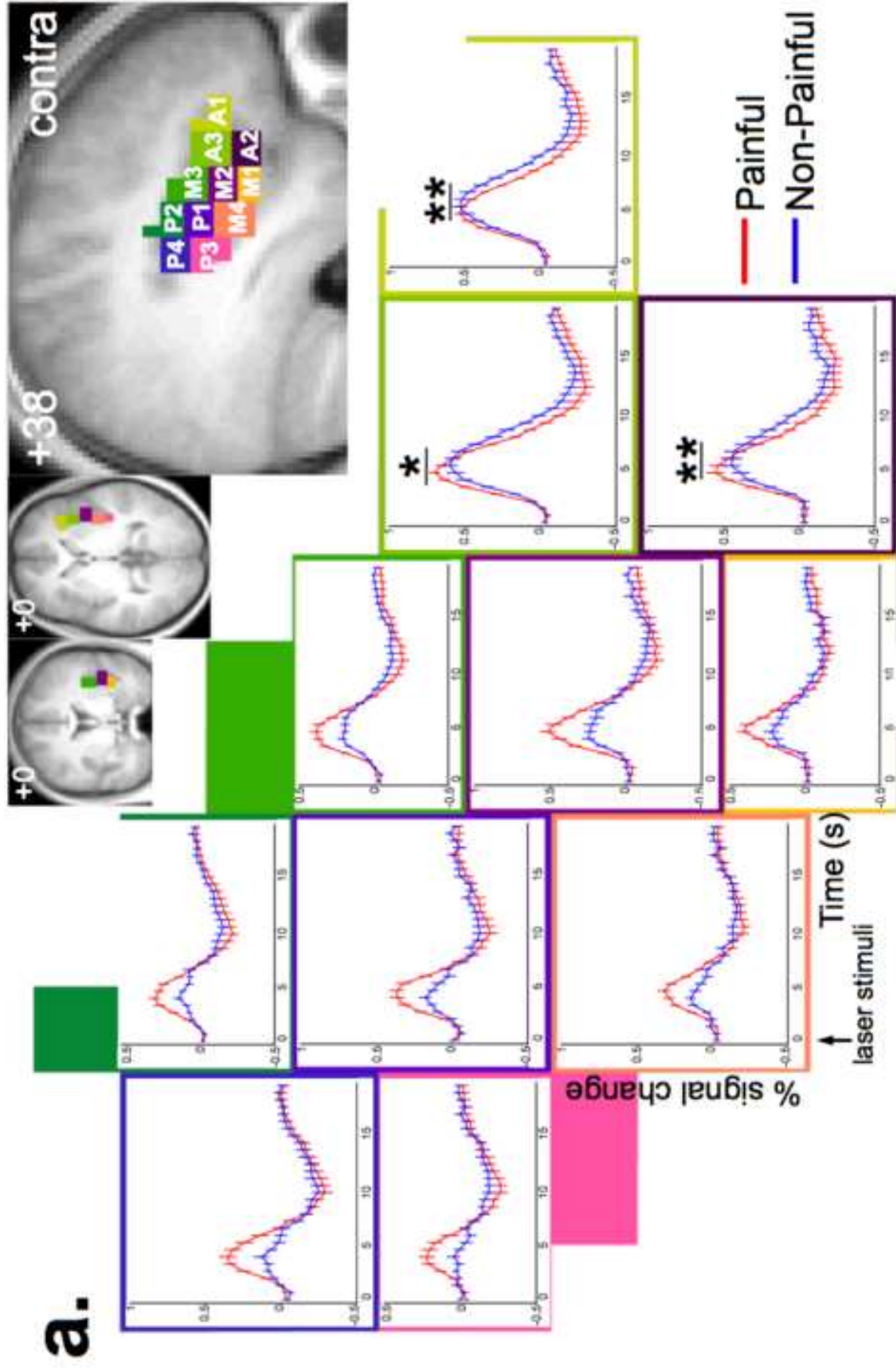


9. Figure 2

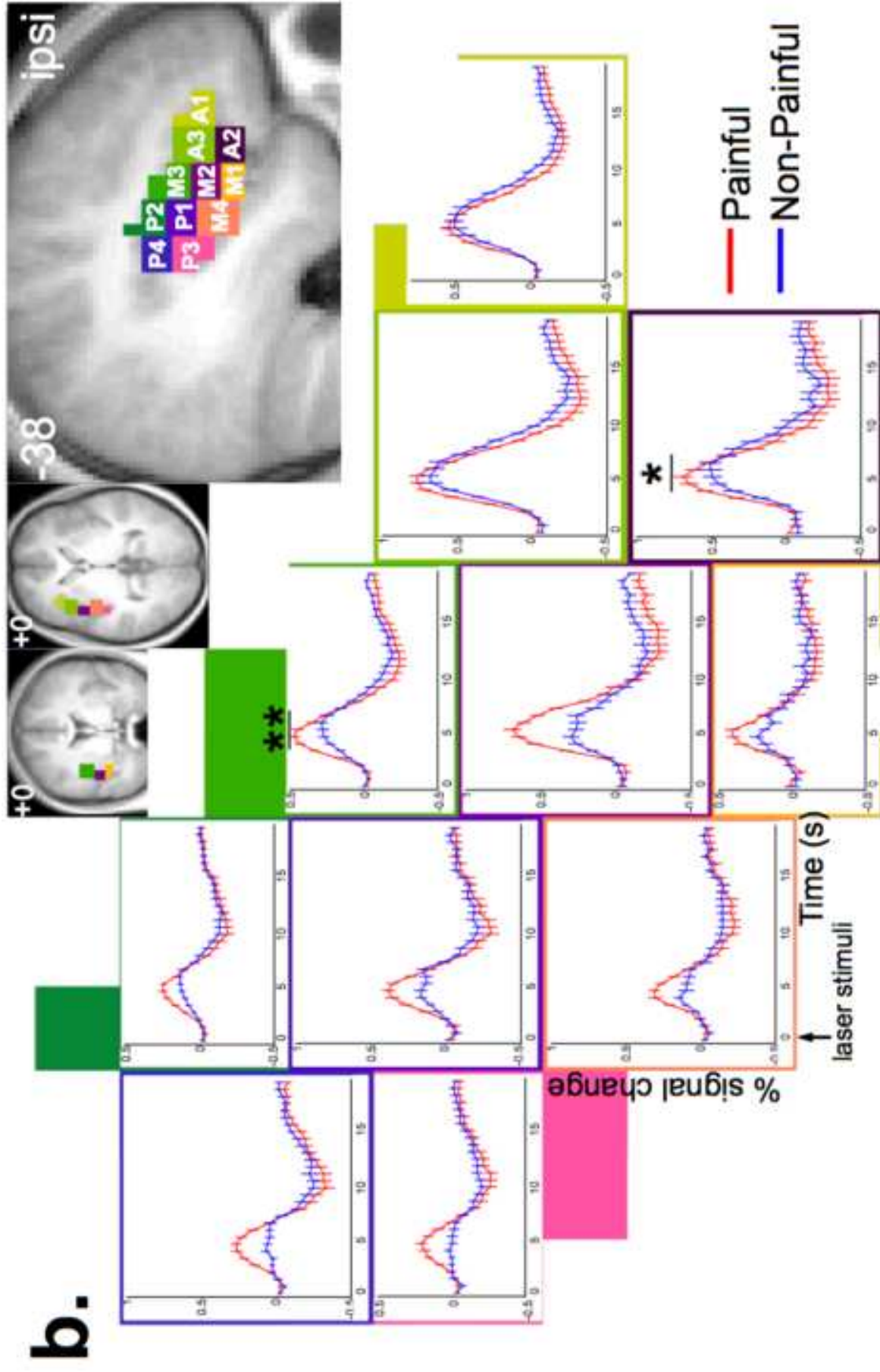
[Click here to download high resolution image](#)



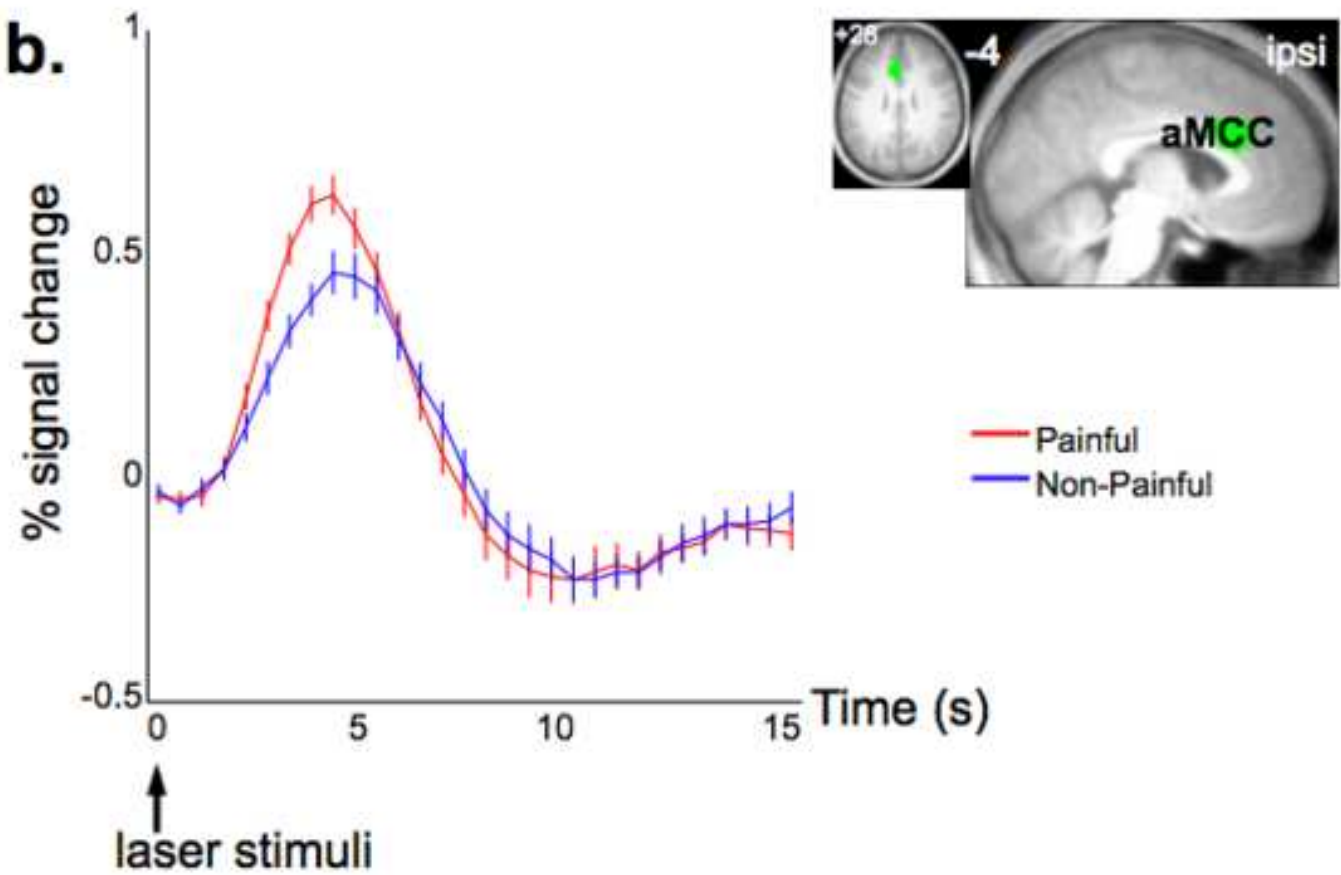
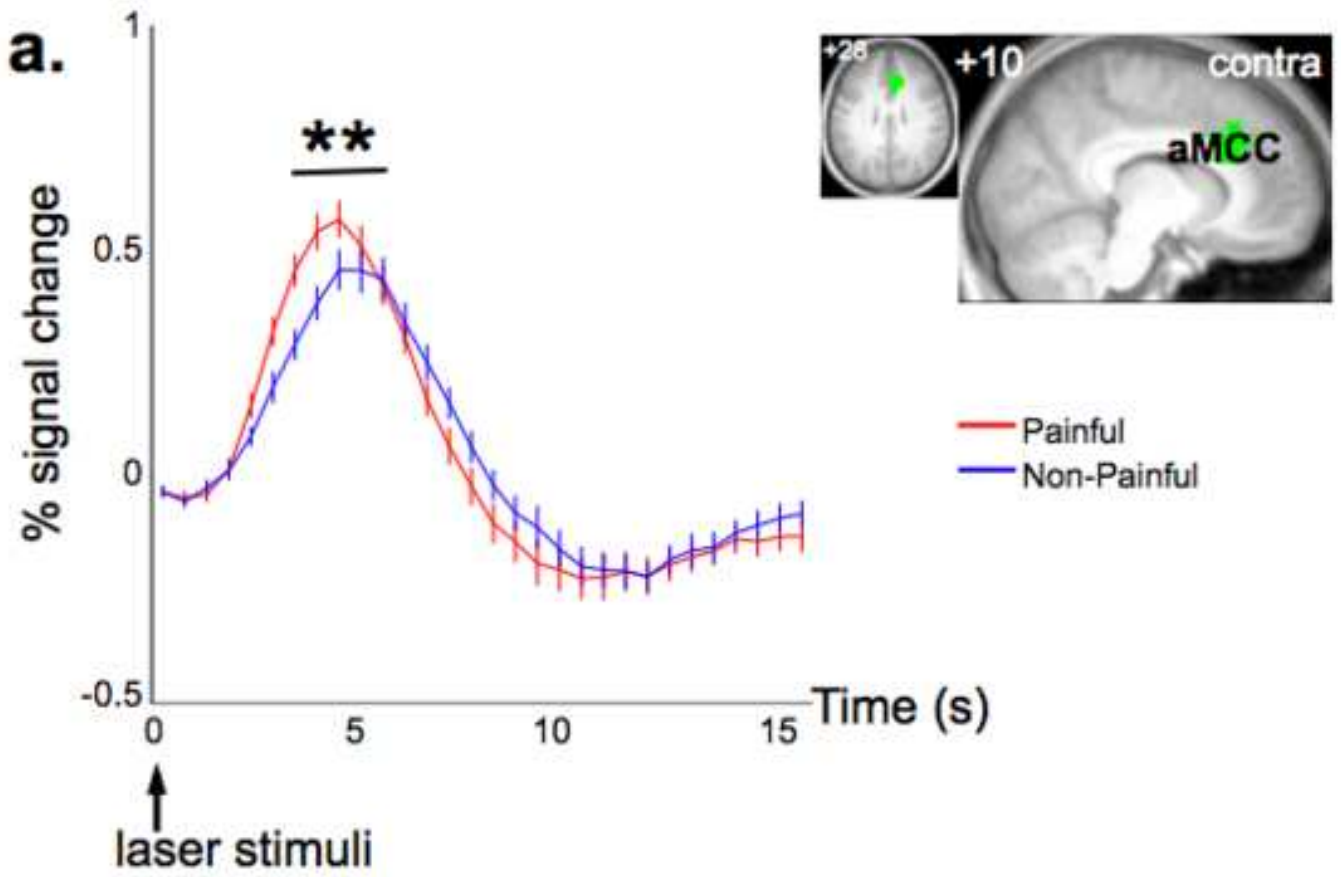
9. Figure 3a
[Click here to download high resolution image](#)



9. Figure 3b
Click here to download high resolution image

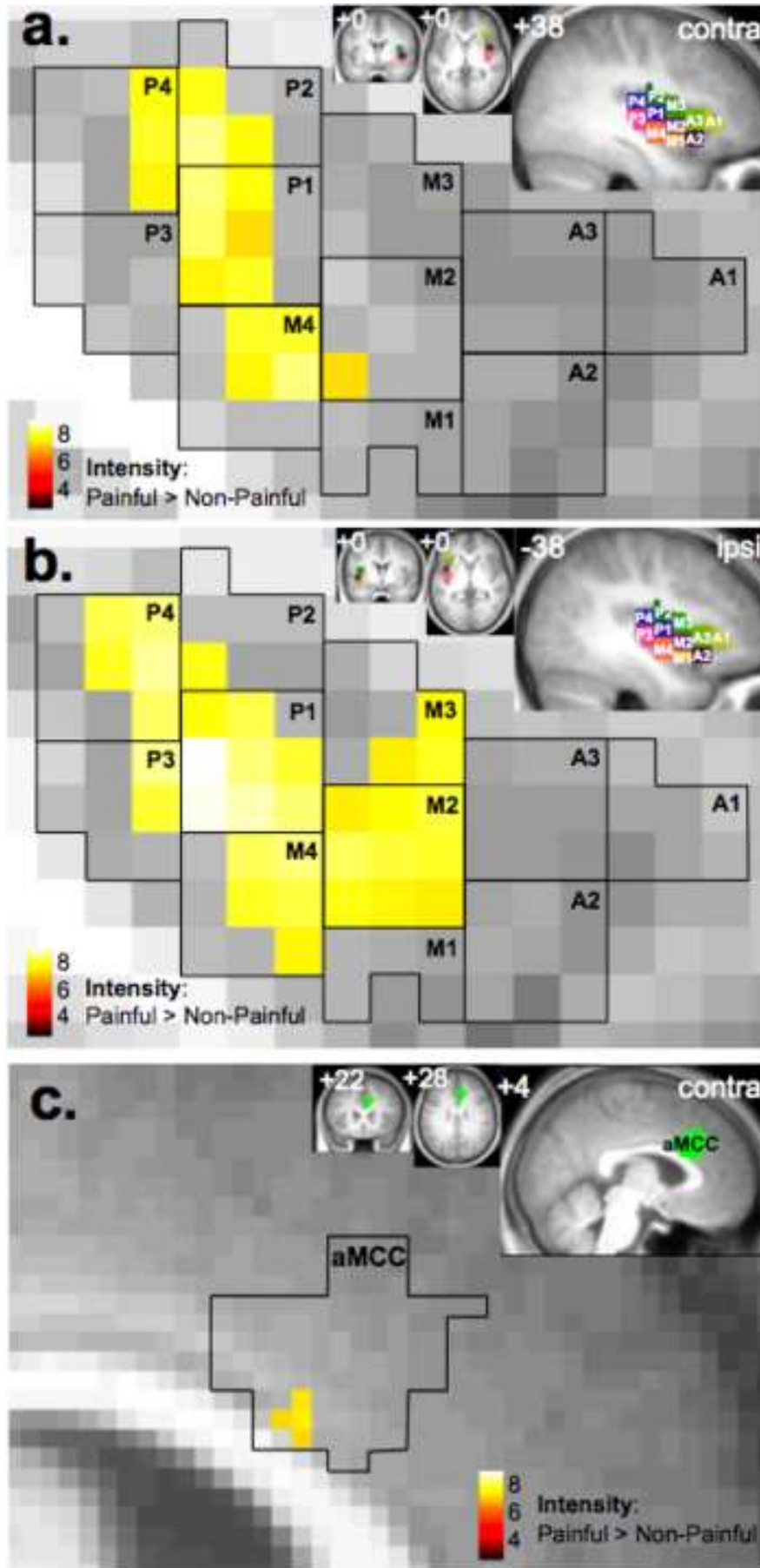


9. Figure 4
[Click here to download high resolution image](#)

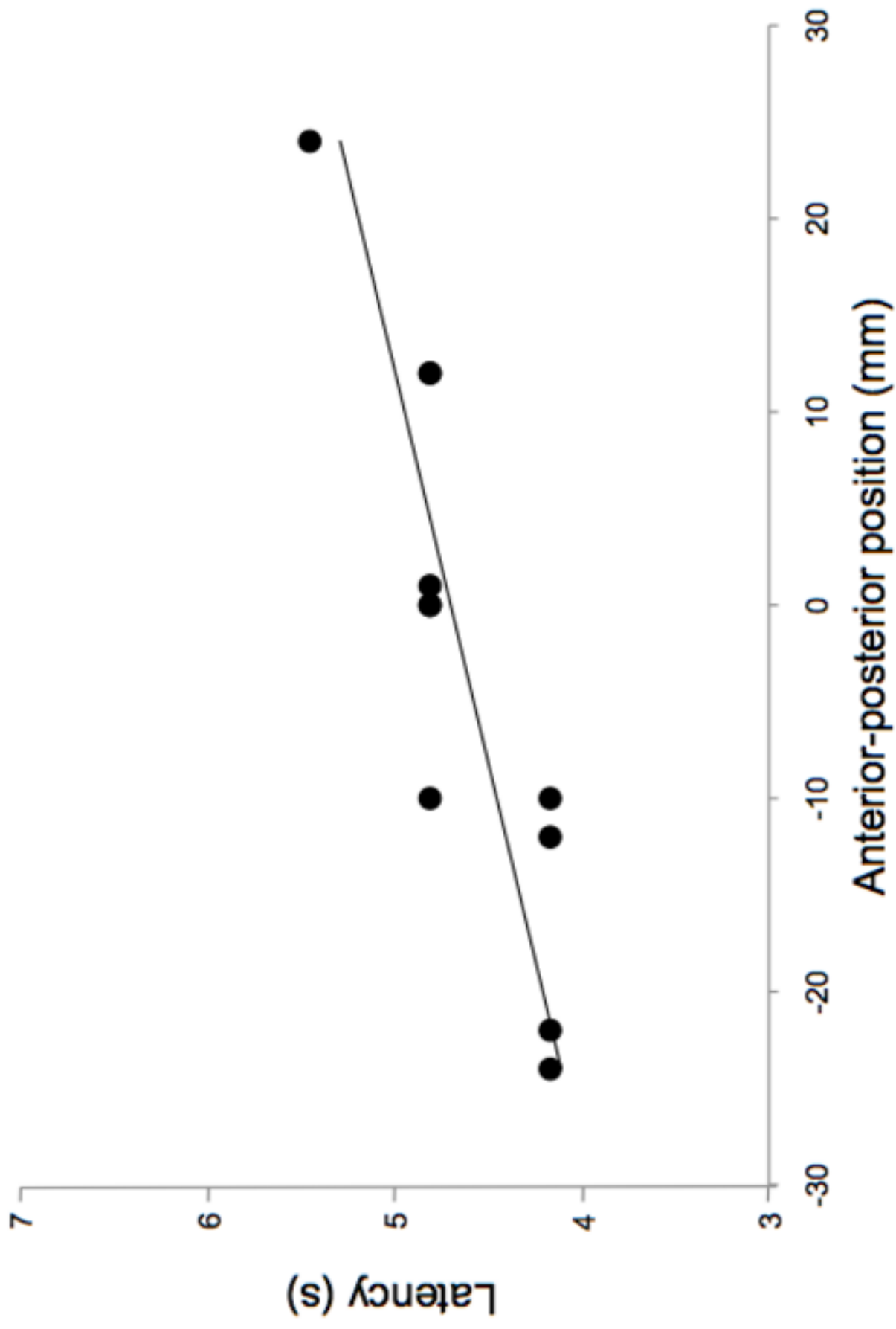


9. Figure 5

[Click here to download high resolution image](#)



9. Figure 6
[Click here to download high resolution image](#)



9. Figure 7
[Click here to download high resolution image](#)

